

Projective Quantum Eigensolver with Generalized Operators

Dibyendu Mondal,¹ Chayan Patra,¹ Dipanjali Halder,¹ and Rahul Maitra^{1,2, a)}

¹⁾Department of Chemistry, Indian Institute of Technology Bombay

Powai, Mumbai 400076, India

²⁾Centre of Excellence in Quantum Information, Computing, Science & Technology,

Indian Institute of Technology Bombay,

Powai, Mumbai 400076, India

Determination of molecular energetics and properties is one of the core challenges in the near-term quantum computing. To this end, hybrid quantum-classical algorithms are preferred for Noisy Intermediate Scale Quantum (NISQ) architectures. The Projective Quantum Eigensolver (PQE) is one such algorithm that optimizes the parameters of the chemistry-inspired unitary coupled cluster (UCC) ansatz using a conventional coupled cluster-like residual minimization. Such a strategy involves the projection of the Schrodinger equation on to linearly independent basis towards the parameter optimization, restricting the ansatz is solely defined in terms of the *excitation* operators. This warrants the inclusion of high-rank operators for strongly correlated systems, leading to increased utilization of quantum resources. In this manuscript, we develop a methodology for determining the generalized operators in terms of a closed form residual equations in the PQE framework that can be efficiently implemented in a quantum computer with manageable quantum resources. Such a strategy requires the removal of the underlying redundancy in high-rank excited determinants, generated due to the presence of the generalized operators in the ansatz, by projecting them on to an internally contracted lower dimensional manifold. With the application on several molecular systems, we have demonstrated our ansatz achieves similar accuracy to the (disentangled) UCC with singles, doubles and triples (SDT) ansatz, while utilizing an order of magnitude fewer quantum gates. Furthermore, when simulated under stochastic Gaussian noise or depolarizing hardware noise, our method shows significantly improved noise resilience compared to the other members of PQE family and the state-of-the-art variational quantum eigensolver.

I. INTRODUCTION

Recent advancements in quantum information and quantum technology have stimulated a great deal of interest in the development of quantum algorithms to solve certain class of classically intractable problems. Determination of molecular energetics is one of such problems due to the exponential growth of the Hilbert-space^{1,2}. Quantum computers on the other hand, with its principle of superposition and entanglement, can handle such problems in a tractable manner. Along this line, various classes of hybrid quantum classical algorithms have gained significant attention for the determination of molecular energetics on the Noisy Intermediate Scale Quantum (NISQ) architecture^{3,4}. The Variational Quantum Eigensolver (VQE)⁵ is the most popular hybrid quantum classical-algorithm for the simulation of many-body systems in the NISQ architectures where the associated wavefunction parameters are optimized in a classical computer to minimize the energy expectation value. While the accuracy critically depends on the expressibility of the chosen ansatz, the unitary coupled cluster (UCC)^{6,7} provides a chemistry-inspired parametrization of unitary operators in terms of the anti-hermitian cluster operators that are proved to be highly accurate. Given the trainability issue of such an ansatz and the disruptive noise profile of the NISQ devices, the VQE algorithms often suffer from issues like slow convergence due to inaccurate determination of energies and gradients, and large scale non-linear nature of the optimization landscape. These issues are further amplified under noise as the num-

ber of quantum measurements required for operator averaging continues to grow. Substantial progress has been made in reducing the number of measurements required for operator averaging by grouping commuting Pauli operators⁸⁻¹², leveraging integral factorization techniques¹³ and employing efficiently computable components¹⁴⁻¹⁶ of the operator. Furthermore, advancements have been achieved in calculating analytical gradients on quantum hardware, utilizing techniques like the parameter-shift rule^{17,18} and its lower-cost variants¹⁹. These approaches have made gradient-based VQE calculations increasingly more feasible on NISQ devices.

A different approach of hybrid quantum-classical algorithm, the Projective Quantum Eigensolver (PQE)²⁰, has emerged as a novel paradigm to solve quantum chemical problems in quantum computers by adopting the unique strategy of optimizing the parameters through classical coupled cluster-like residual minimization. It was previously observed that the convergence pattern of PQE is more rapid than VQE even in presence of noise. Consequently, when started with a fixed structured ansatz, VQE warrants more gradient evaluations compared to the corresponding residual evaluations required by PQE²⁰. Thus within PQE framework, one must aim to minimize the number of requisite residual evaluations in order to minimize the utilization of quantum resources. Within the disentangled Unitary Coupled Cluster (dUCC) framework²¹, PQE determines residual elements by projecting through each of the singly, doubly, or higher-order excited determinants generated by the action of cluster operators on the reference Hartree-Fock (HF) state. For systems with low to moderate electronic correlation effects, dUCC ansatz with singles and doubles can provide a good quantitative accuracy with respect to Full Configuration Interaction (FCI) energies. However, in systems with strong correlation, it becomes necessary to in-

^{a)}Electronic mail: r.maitra@chem.iitb.ac.in

clude triples or higher-order excitations to accurately capture correlation effects. This inclusion demands a higher number of quantum resources, particularly in terms of the number of entangling quantum gates, which poses prohibitive challenges for current NISQ devices. Several low-cost variants of PQE and Selected PQE (SPQE) have recently been formulated such as– the CNOT-efficient PQE²² that uses qubit-excitation operators²³, methods of moments²⁴ inspired PQE²⁵ and adiabatically decoupled PQE^{26,27} as well as its dynamic variant with auxiliary subspace corrections²⁸ where the principles of adiabatic decoupling^{29,30} is adopted - to mention a few. Although these variants of PQE can extensively limit the resource-requirements such as the CNOT counts and measurements, none of them theoretically guarantees the exclusion of explicit triples and higher-order excitation operators (which typically proliferates the circuit depth in an uncontrollable manner) from the ansatz. A potential solution to this issue has been addressed within the VQE framework. This involves incorporating two-body generalized operators (\hat{G}) into the ansatz^{31,32}, which can implicitly account for higher-order excitation effects through lower rank tensor decomposition. However, while optimizing the generalized operators in VQE framework is straightforward, their incorporation in the PQE imposes significant theoretical challenges. This is due to the fact that the action of these two-body generalized operators \hat{G} on the reference HF state is nilpotent, giving rise to their Vacuum Annihilating Condition (VAC): $\hat{G}|\phi_0\rangle = 0$, where $|\phi_0\rangle$ is the HF reference. This characteristic makes it particularly challenging to derive a direct closed-form expression for determining residual elements associated with these generalized operators in the PQE framework.

In this manuscript, we focus on a specific set of two-body generalized operators known as scattering operators^{33–36}, which implicitly generate higher-order excitation effects when acting on top of low-order excited determinants. The choice of such an operator and the structure of the ansatz, although not the key focus of this manuscript, have been briefly justified in the subsequent sections and can also be found elsewhere. As the primary objective of this paper, starting from an arbitrarily structured ansatz containing such generalized operators, we have developed a novel approach to derive a closed-form equation for determining their residual elements that can easily be implemented in quantum computers with minimal quantum resources. This algorithm will be referred to as generalized PQE (GPQE)– an abbreviation we will be using throughout the manuscript. Such an undertaking bypasses the need of explicit incorporation of higher order cluster operators within the traditional PQE framework at the cost of prohibitively high quantum resources, but are otherwise impossible to exclude in strong correlation regime. We also demonstrate that GPQE retains all the advantageous features of the traditional PQE, particularly its superior resilience to hardware noise, over VQE. With a brief summary of the conventional PQE, its selected variant (SPQE) and their associated scaling, we motivate the readers to the importance of a disentangled ansatz containing the scatterers. We derive our projective formulation, GPQE, in Sec. II C where we introduce an internally contracted projection manifold for reaching to a closed-shell expression of the

scattering residuals. We have demonstrated its accuracy and resource efficiency in Sec. III in ideal (noiseless) as well as in noisy environment, and have convincingly affirmed its superiority over other members of the conventional PQE family as well as VQE. Finally we conclude in Sec. IV.

II. THEORY

A. A Brief Summary of Conventional Projective Quantum Eigensolver and its Variants

PQE relies on the construction of a parametrized trial wavefunction $|\Psi(\theta)\rangle$ via the action of a parametrized ansatz $\hat{U}(\theta)$ on the Hartree-Fock (HF) reference state ($|\phi_0\rangle$): $|\Psi(\theta)\rangle = \hat{U}(\theta)|\phi_0\rangle$. In general one chooses $\hat{U}(\theta)$ to be the disentangled unitary coupled cluster (dUCC) ansatz:

$$\hat{U}(\theta) = \prod_{\mu} e^{\hat{\kappa}_{\mu}(\theta_{\mu})} \quad (1)$$

where, $\hat{\kappa}_{\mu}(\theta_{\mu}) = \hat{\tau}_{\mu}(\theta_{\mu}) - \hat{\tau}_{\mu}^{\dagger}(\theta_{\mu})$ is an anti-hermitian cluster operator with $\hat{\tau}_{\mu}(\theta_{\mu}) = \theta_{\mu} \hat{Y}_{\mu} = \theta_{ij\dots}^{ab\dots} (\hat{a}_a^{\dagger} \hat{a}_b^{\dagger} \dots \hat{a}_j \hat{a}_i)$ and θ_{μ} being the associated parameter. Here, μ denotes a multi-indexed composite hole-particle *excitation* label of arbitrary order (single, double, triple or higher order) containing the indices i, j, \dots (a, b, \dots) that refer to the occupied (unoccupied) spinorbitals in the HF reference. To distinguish between the various order of excitation operators, we use the notations $\bar{I}, \bar{J}, \bar{K} \dots$ for single excitation operators, $I, J, K \dots$ for double excitation operators and $X, Y, Z \dots$ for triple excitation operators. This notation is consistently employed throughout the manuscript. Unlike VQE, PQE adopts a projective approach leveraging traditional coupled-cluster-like quasi-Newton technique to iteratively optimize the parameters:

$$\theta_{\mu}^{(n+1)} = \theta_{\mu}^{(n)} + \frac{r_{\mu}^{(n)}}{D_{\mu}} \quad (2)$$

Here, n is the iterative step counter and D_{μ} is the standard Møller-Plesset denominator, $D_{\mu} = \varepsilon_i + \varepsilon_j + \dots - \varepsilon_a - \varepsilon_b \dots$, where the ε_i are Hartree-Fock orbital energies. In Eq. (2), r_{μ} is the residual element which can be constructed as the off-diagonal matrix elements of a similarity transformed Hamiltonian $\bar{H} = \hat{U}^{\dagger}(\theta) \hat{H} \hat{U}(\theta)$ between the excited determinants $|\phi_{\mu}\rangle$ s and the reference $|\phi_0\rangle$:

$$r_{\mu}(\theta) = \langle \phi_{\mu} | \hat{U}^{\dagger}(\theta) \hat{H} \hat{U}(\theta) | \phi_0 \rangle; \mu \neq 0. \quad (3)$$

Such a projection allows us to have exactly same number of unknown parameters as the number of the truncated set of excited determinants. The residuals can be efficiently calculated using a quantum computer as they can be further expressed as a sum of three diagonal quantities:

$$r_{\mu} = \langle \Omega_{\mu}(\frac{\pi}{4}) | \bar{H} | \Omega_{\mu}(\frac{\pi}{4}) \rangle - \frac{1}{2} E_{\mu} - \frac{1}{2} E_0 \quad (4)$$

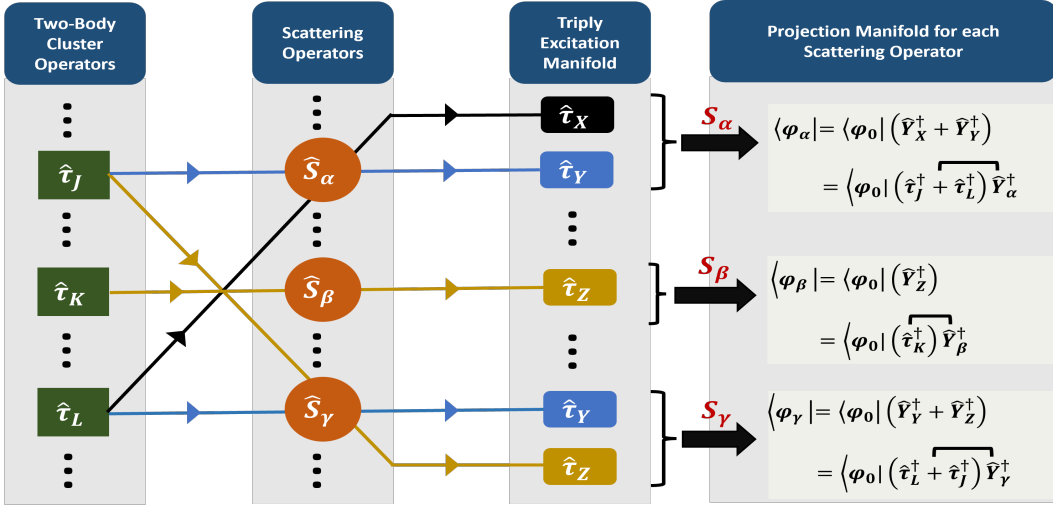


FIG. 1: Schematic representation of projection manifold for scattering operators

where, $|\Omega_\mu(\theta)\rangle = e^{\hat{\kappa}_\mu(\theta)}|\phi_0\rangle$, $E_\mu = \langle\phi_\mu|\hat{H}|\phi_\mu\rangle$ and $E_0 = \langle\phi_0|\hat{H}|\phi_0\rangle$. This iterative process converges when the *residual condition* $r_\mu \rightarrow 0$ is satisfied. From the definition of Eq.(3) it is evident that residuals are nothing but those non-diagonal elements that form a column (or row) of the matrix representation of \hat{H} in the many-body determinantal basis. As a consequence of this structure, the Gershgorin's circle theorem guarantees that the energy error (ΔE) between the exact ground state energy (E_{exact}) and ground state energy obtained by PQE (E_{PQE}) is bounded by $\Delta E = |E_{exact} - E_{PQE}| \leq \rho = \sum_{\mu \neq 0} r_\mu$. Here, $\rho = \sum_{\mu \neq 0} r_\mu$ is the radius of the Gershgorin's circle and the summation includes only those residuals for which the residual condition is not enforced. It is crucial to note that the conventional PQE necessitates the presence of *only excitation-type operators* (\hat{Y}_μ) in the dUCC ansatz such that $\hat{Y}_\mu|\phi_0\rangle \rightarrow |\phi_\mu\rangle$. This leads to an unwanted restriction on the operator pool to construct $\hat{U}(\theta)$: it is warranted that high rank excitation operators must be included in $\hat{U}(\theta)$ for strongly correlated systems (and such high rank connected excitation operators cannot be decomposed into lower rank operators), leading to an impractical proliferation of circuit depth towards NISQ realization.

The associated dynamic quantum algorithm in the PQE paradigm, known as selected PQE (SPQE)²⁰, is based upon an “evolve-and-measure” technique that involves a series of alternating macro- and micro-iteration cycles. In the macro-iteration steps a low-rank decomposition³⁷ of the Hamiltonian is used to get a *residual state* via time evolution for a short-period Δt . This residual state is subsequently measured to filter a set of “important” determinants (and excitation operators) of pre-defined ranks governed by a macro-iteration threshold ω to construct a compact ansatz. The parameters associated with these specific important excitation operators are then optimized via PQE micro-iteration cycles. For more theoretical and algorithmic details of SPQE and the associated resource efficient variants we refer to the paper by Stair *et al.*²⁰ along with some of our recently developed works^{26,28}.

However, like the parent PQE, its selected variant is also restricted to include only the excitation operators and as such its generalization to incorporate other class of vacuum annihilating operators require further theoretical development as we described below.

B. Projective Quantum Eigensolver with Generalized Operators: Choice of the Ansatz and Theoretical Challenges

The idea of expressing a many-electronic wavefunction in terms of the generalized operators stems from the seminal works by Nooijen³⁸ and Nakatsuji³⁹. The subsequent unitary adaptation has motivated its implementation in the quantum architecture. Following the concepts of contracted Schrodinger's equations⁴⁰, some of the present authors have previously put forward the notion of dual exponential unitary in terms of one and two-body cluster operators and a subset of generalized operators for improved expressibility of quantum ansatz^{32,41}. In general, such an ansatz may be expressed as:

$$e^{\hat{\lambda}} e^{\hat{\kappa}} = \prod_{\alpha} e^{\hat{\lambda}_{\alpha}(\theta_{\alpha})} \prod_I e^{\hat{\kappa}_I(\theta_I)} \quad (5)$$

which spans the N-electron Hilbert space via nested commutators:

$$e^{\hat{\lambda}} e^{\hat{\kappa}} = e^{\hat{\lambda} + \hat{\kappa} + [\hat{\lambda}, \hat{\kappa}] + [\hat{\lambda}, [\hat{\lambda}, \hat{\kappa}]] + \dots} \quad (6)$$

Structurally, the choice of $\hat{\lambda} = \hat{G} - \hat{G}^\dagger$ plays a pivotal role in deciphering the expressibility and accuracy of the ansatz with the following two categories:

1. Type-1: \hat{G} is chosen to be two-body operator with effective hole-particle rank of one and have one quasi-orbital destruction.
2. Type-2: \hat{G} is chosen to be two-body operator with effective hole-particle rank of zero and have two quasi-orbital destruction.

Note that due to the presence of at least one quasi-orbital *destruction* operator, both of these set of operators satisfy the VAC: $\hat{G}|\phi_0\rangle = 0$ (and that is the reason their implementation in the PQE framework is highly non-trivial irrespective of their position in the ansatz). While in this manuscript, we do not aim to optimize the circuit implementation, and thus we will not be making any comparative analysis between the two choices stated above; rather, we will start with an ansatz of the form expressed by Eq.(5) and would choose λ to be composed of Type-1 \hat{G} operators such that their rank increasing action leads to a better span of the N -electron Hilbert space⁴¹. Thus our motivation is to start with an ansatz of structure like that in Eq.(5) and develop the theoretical methodology to solve within PQE framework so that the advantages of PQE is retained while at the same time a desired accuracy may be achieved with less quantum resources. Here we start with some further discussions about \hat{G} (of Type-1) that will motivate us toward our development. We will refer to these specific operators (\hat{G} of Type-1) as *scatterer* and denote it as \hat{S} .

The scatterers are a class of generalized two-body operators with one quasi-orbital destruction operator and depending on whether such destruction operators are hole or particle type, we designate them as \hat{S}_h and \hat{S}_p respectively: $\hat{S} = \hat{S}_h + \hat{S}_p$

$$\begin{aligned}\hat{S}_h &= \frac{1}{2}\theta_\alpha\hat{Y}_\alpha = \frac{1}{2}\theta_{i,j}^{a,m}\hat{a}_a^\dagger\hat{a}_m^\dagger\hat{a}_j\hat{a}_i \\ \hat{S}_p &= \frac{1}{2}\theta_\beta\hat{Y}_\beta = \frac{1}{2}\theta_{i,e}^{a,b}\hat{a}_a^\dagger\hat{a}_e^\dagger\hat{a}_e\hat{a}_i\end{aligned}\quad (7)$$

Here α, β are the composite indices associated with the orbital indices of \hat{S} . The indices m and e refer to a set of occupied (hole) and unoccupied (particle) spinorbitals in the reference HF state, and they together form a contractible set of orbitals (CSOs). The essential difference between the cluster and scattering operators lies in their action on the reference determinant: while the action of $\hat{\tau}$ on the reference HF determinant generates an excited determinant, the action of scatterer leads to annihilation of the reference leading to the VAC: $\hat{S}|\phi_0\rangle = 0$. The non-commutativity between the cluster operators and scatterers is exploited to simulate connected higher order excitations:

$$\sum_m \hat{S}_{k,j}^{c,m} \hat{\tau}_{i,m}^{a,b} \rightarrow \hat{\tau}_{i,j,k}^{a,b,c}, \sum_e \hat{S}_{k,e}^{c,b} \hat{\tau}_{i,j}^{a,e} \rightarrow \hat{\tau}_{i,j,k}^{a,b,c} \quad (8)$$

As the scattering operators have an effective hole-particle excitation rank one, each such contraction between $\hat{\tau}$ and \hat{S} increases the excitation rank by one: $\hat{S}\hat{\tau}_2 \rightarrow \hat{\tau}_3, \hat{S}\hat{S}\hat{\tau}_2 \rightarrow \hat{\tau}_4 \dots$. However, such a lower rank decomposition of the higher rank excitations may often lead to redundant description (*vide infra*). This condition, coupled with the associated VAC makes a projective formulation to determine the corresponding scatterer rotations highly nontrivial.

C. Towards the Construction of Residue Equation for Scattering Operators

The discussion in the preceding section suggests that the scattering operators cannot be determined directly by a projective formulation due to the associated VAC. However, noting these scatterers have non-zero action on certain doubly excited determinants leading to the three body excited determinants, in principle, such operators may be determined by computing the matrix elements of an effective Hamiltonian operator between a triply and certain doubly excited determinant via Hadamard tests. However, projection by triply excited determinants often leads to over-determinedness of the scattering amplitudes, as we explain below.

When the three-body cluster operators are explicitly included in the ansatz, the number of projections by triply excited determinants are precisely equal to the number of unknown three-body parameters. However, when such a triple excitation is decomposed into a tensor product of two two-body operators (like scatterers and the cluster operators), such one-to-one mapping between the number of triply excited determinants ($O(n_o^3 n_v^3)$) and the number of unknown parameters ($O(n_o^2 n_o^{CSO} n_v + n_o n_v^{CSO} n_v^2)$) no longer exists. This arises from the fact that the action of the scattering operators on various two-body excited determinants may lead to the redundant generation of triply excited determinants: each such three-body cluster operator may be generated by more than one combinations of \hat{Y}_α and \hat{Y}_I . Also, this implies that each element \hat{Y}_α may get coupled with different \hat{Y}_I 's (depending on the commonality of CSO) to generate different \hat{Y}_X :

$$\sum_I (\hat{Y}_\alpha \hat{Y}_I) |\phi_0\rangle = \sum_X \hat{Y}_X |\phi_0\rangle \rightarrow \sum_X |\phi_X\rangle \quad (9)$$

where we have deliberately put the explicit summation over I for clarity. This implies that the structure of \hat{Y}_α is subsumed in each such effective three-body excitation operator \hat{Y}_X . Furthermore, the sum over the triply excited determinants arises due to the internal summation over various \hat{Y}_I 's, each sharing a common CSO with \hat{Y}_α . Thus the direct determination the effective hamiltonian matrix elements between the triply and doubly excited determinants is theoretically wrong as they have unequal number of such matrix elements as the number of unknowns, and one needs to judiciously contract the three-body projection manifold such that the number of projections equals the number of unknown parameters.

In order to bypass the redundancy, we propose a basis transformation to a lower dimensional manifold in which a contracted basis vector $|\phi_\alpha\rangle$ is obtained by transforming the $|\phi_X\rangle$ basis via a rectangular matrix such that

$$|\phi_\alpha\rangle = \sum_I \theta_I (\hat{Y}_\alpha \hat{Y}_I) |\phi_0\rangle = \sum_X C_{\alpha X} |\phi_X\rangle \quad (10)$$

where, $C_{\alpha X}$ is a rectangular transformation matrix. Here in Eq.(10), for a particular α only those elements in the transformation matrix $C_{\alpha X}$ are non-zero for which \hat{Y}_α is structurally a subpart of \hat{Y}_X . This implies that the associated $|\phi_X\rangle$ may

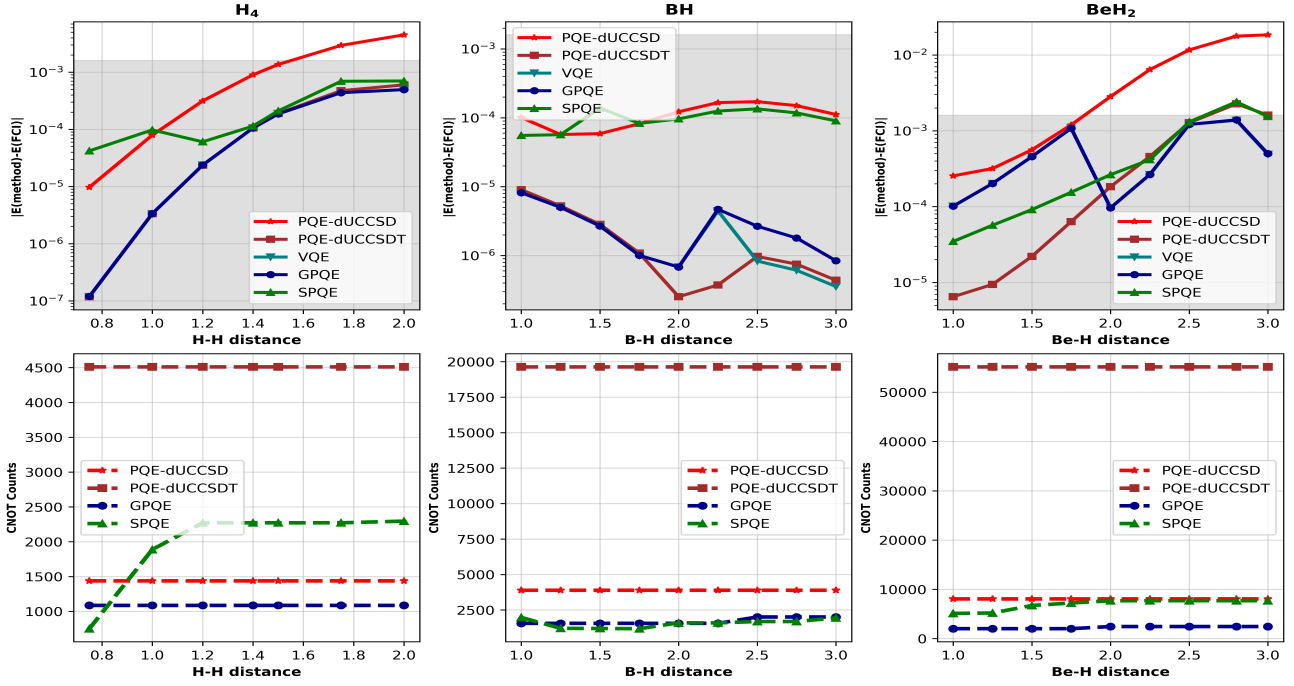


FIG. 2: Energy difference profile (from FCI, in logarithm scale, along the first row) and CNOT gate count (along the second row) for our GPQE, PQE-dUCCSD, PQE-dUCCSDT, SPQE (with SDT pool) and VQE over the potential energy surface. The shaded region indicates the chemical accuracy. Please note that the same ansatz is used for both GPQE and VQE and their results are nearly identical.

be obtained via tensor contraction between \hat{Y}_α and the corresponding \hat{Y}_I s. In this sense, it is a dimensionality reduction approach via a transformation to a lower dimensional basis:

$$\{|\phi_S\rangle, |\phi_D\rangle, |\phi_X\rangle\} \rightarrow \{|\phi_S\rangle, |\phi_D\rangle, |\phi_\alpha\rangle\} \quad (11)$$

such that $\dim(|\phi_\alpha\rangle)$ is $O(n_o^2 n_v^{CSO} n_v + n_o n_v^{CSO} n_v^2)$ which is $\ll \dim(|\phi_X\rangle)$ having $O(n_o^3 n_v^3)$ elements.

With the knowledge of θ_I 's obtained via Eq.(2) with an ansatz $\hat{U}(\theta) = \prod_\alpha e^{\hat{\sigma}_\alpha(\theta_\alpha)} \prod_I e^{\hat{\kappa}_I(\theta_I)}$, where $\hat{\sigma}_\alpha = \hat{S}_\alpha - \hat{S}_\alpha^\dagger$, we construct a residue for \hat{S}_α by explicitly taking the matrix element of $\bar{H} = \hat{U}^\dagger(\theta) \hat{H} \hat{U}(\theta)$ between the reference $|\phi_0\rangle$ and a set of contracted triply excited determinants $\sum_I \langle \phi_0 | (\hat{Y}_I^\dagger \hat{Y}_\alpha^\dagger) \theta_I$ which effectively spans the transformed lower dimensional manifold $\{|\phi_\alpha\rangle\}$.

$$r_\alpha(\theta) = \sum_I \theta_I \langle \phi_0 | (\hat{Y}_I^\dagger \hat{Y}_\alpha^\dagger) \hat{U}^\dagger(\theta) \hat{H} \hat{U}(\theta) | \phi_0 \rangle \quad (12)$$

The summation over the index I is equivalent to a restricted summation over the resultant three-body excitations X as Eq. 9. Hence in this lower dimensional basis, residuals r_α are basically the non-diagonal column (or row) elements of the matrix representation of the similarity transformed Hamiltonian $\bar{H} = \hat{U}^\dagger(\theta) \hat{H} \hat{U}(\theta)$.

Following the conventional approach, the above expression can be further broken down into the sums of three diagonal terms which can efficiently be determined in quantum com-

puters:

$$r_\alpha(\theta) = \sum_{I:(I\alpha \rightarrow X)} \theta_I \left(\langle \Omega_X(\frac{\pi}{4}) | \bar{H} | \Omega_X(\frac{\pi}{4}) \rangle - \frac{1}{2} E_X - \frac{1}{2} E_0 \right) \quad (13)$$

where the terms have their usual meaning as defined in Sec. II A. The residue corresponding to \hat{S}_α now has a particularly simple structure: it is structurally akin to the residue for cluster operators, however, each such residual is explicitly summed over all the three-body excitation terms that has the common \hat{Y}_α subsumed in it. The presence of the associated θ_I 's ensures that the ‘‘contracted’’ projection manifold is weighted by all the underlying two-body determinants on which the particular \hat{Y}_α has a non-vanishing action.

Following the construction of the residue via its projection against the contracted excited determinants, the scattering amplitudes may be iteratively updated using the usual quasi-Newton scheme:

$$\theta_\alpha^{(n+1)} = \theta_\alpha^{(n)} + \frac{r_\alpha^{(n)}(\theta)}{D_\alpha} \quad (14)$$

where D_α denotes the local Møller-Plesset denominator for a \hat{S}_α . Eq. (2) and (14) together generate a set of coupled equations that are iteratively solved to obtain the converged parameters. With this, we move to the next section where we discuss the efficiency of GPQE by comparing against allied PQE based methods and VQE under ideal and noisy environment.

III. RESULTS AND DISCUSSIONS

A. General Considerations

In this work, all implementations were carried out using the Qiskit-Nature interface⁴², which imports one- and two-body integrals as well as orbital energies from PySCF⁴³. We employed the STO-3G basis set⁴⁴ for all the systems with direct spinorbital to qubit mapping. The Jordan-Wigner encoding was used to convert second-quantized fermionic operators into qubit operators⁴⁵. To accelerate the optimization trajectory in PQE framework, the Direct Inversion of the Iterative Subspace (DIIS) was applied⁴⁶. We have used Broyden-Fletcher-Goldfarb-Shannon (BFGS)⁴⁷⁻⁵⁰ algorithm (as implemented in SCIPY⁵¹ library) for VQE optimization. For SPQE calculations we used QForte⁵² with time-evolution parameter $\Delta t = 0.001$ and macro-iteration threshold $\omega = 0.01$, while keeping the maximum excitation rank to order three (i.e. singles, doubles and triples). In order to keep the gate depth to the minimum for our formulation, we selected only certain cluster operators and scatterers as described below. Please note that for an unbiased comparison, both GPQE and the VQE simulations (wherever applicable) employed the same decomposed ansatz.

B. Selection of the dominant operators

To work with the most compact form of the ansatz within the partially disentangled unitary framework, one may judiciously choose certain operators while the seemingly unimportant ones are neglected altogether. For all the two-body operators (\hat{t}_j 's and \hat{S}_α 's), we resort to the corresponding first order perturbative measures to prune the list of the operators: only those operators are chosen for which the absolute magnitude of their first order estimate⁵³ is greater than 10^{-5} . The singles are chosen based on the second order perturbative estimate since they appear in the second order of many-body perturbation theory for the first time. This implies that only those singles are chosen where

$$\left| \text{Amp} \left(\frac{\sqrt{V_\alpha^\dagger V_I \bar{K}}}{D_{\bar{K}} D_I} \right) \right| > 10^{-6} \quad (15)$$

where V denotes the two-electron integrals. Furthermore, with the pruned set of scatterers, only those are retained for which both the quasi-hole or quasi-particle creation operators (for \hat{S}_h and \hat{S}_p , respectively) carry paired orbital labels. Additionally, as demanded by the formulation, the quasi-hole and quasi-particle destruction operators are restricted to only certain orbitals spanning the CSOs.

C. Accuracy and CNOT gate counts over the Potential Energy Surface: Simulation under noiseless environment

In this section, we study the performance and resource efficiency of our method with noiseless simulator, and com-

pared and contrasted our results with PQE-dUCCSD, PQE-dUCCSDT, SPQE (SDT pool). The absolute accuracy of all these methods are measured against Full Configuration Interaction (FCI).

The simultaneous symmetric stretching of all the bonds in linear H_4 chain is a well-studied model system for studying electronic strong-correlation behaviour in quantum many-body theories. In the STO-3G basis, H_4 contains 4 electrons in 8 spinorbitals, which are directly mapped onto 8 qubits. For our study we varied the $H-H$ bond distance (R_{H-H}) from 0.75Å to 2.0Å. For all geometries, we included the HOMO and LUMO spinorbitals in CSOs towards the simulation of triples. As shown in Fig.2, GPQE demonstrates comparable, and in some cases superior accuracy to the PQE-dUCCSDT ansatz, while requiring less than one-third the number of CNOT gates.

The single bond dissociation of $B-H$ is our next test set. With frozen $1s$ orbital of B , it renders to be a system with 4 electrons in 10 spinorbitals. It was observed that for $B-H$ bond lengths ranging from 1.0Å to 2.25Å, there is no low-lying particle orbital through which the scatterer may contract with a selected cluster operator. This essentially means that for these geometries, \hat{S}_p has no role to play and the CSO is constituted by HOMO and (HOMO-1). Beyond $R_{B-H} = 2.25$, the CSO is composed of HOMO and LUMO. Fig.2 (second column) demonstrates the energy profile of GPQE that closely matches with the PQE-dUCCSDT across the PES while the former requiring almost an order fewer CNOT gates than the latter. SPQE with SDT pool utilizes comparable number of CNOT gates with our ansatz, however, at the cost of compromised the accuracy.

The next system in our study involve the symmetric stretching of $Be-H$ bonds in linear BeH_2 . With the $1s$ orbital of Be frozen, it has 4 electrons in 12 spinorbitals. For symmetry considerations, the CSO contains HOMO and (HOMO-1) up to $R_{Be-H} = 1.75$ Å, while it involves HOMO and LUMO beyond this point. The energy accuracy obtained from our ansatz is significantly better than dUCCSD across the potential energy surface, even while using less than one-third of the CNOT gates than the latter. As shown in the Fig.2 (third column), for the initial few points, SPQE (with the SDT pool) and dUCCSDT ansatz provide somewhat better accuracy than GPQE. However, the corresponding CNOT counts for SPQE and PQE-dUCCSDT are almost double and an order of magnitude higher compared to GPQE, respectively. Interestingly, in the strongly correlated regions, the accuracy of GPQE surpasses both SPQE and PQE-dUCCSDT, as demonstrated in the figure.

At this stage, one may note that in the present approach, we have worked with an ansatz of the form given in Eq. 5 where all the scatterers act after the action of all the cluster operators. In both the cases, the operators are taken in lexical ordering where the one body cluster operators act first on the reference, followed by the two body cluster operators and finally by the scatterers. However, one may also choose to work with a differently ordered ansatz where the appearance of the scatterers and the cluster operators are interwoven⁵³⁻⁵⁵. We point out that in such cases, our solution strategy for both set of the parameters remains unchanged as long as each of the

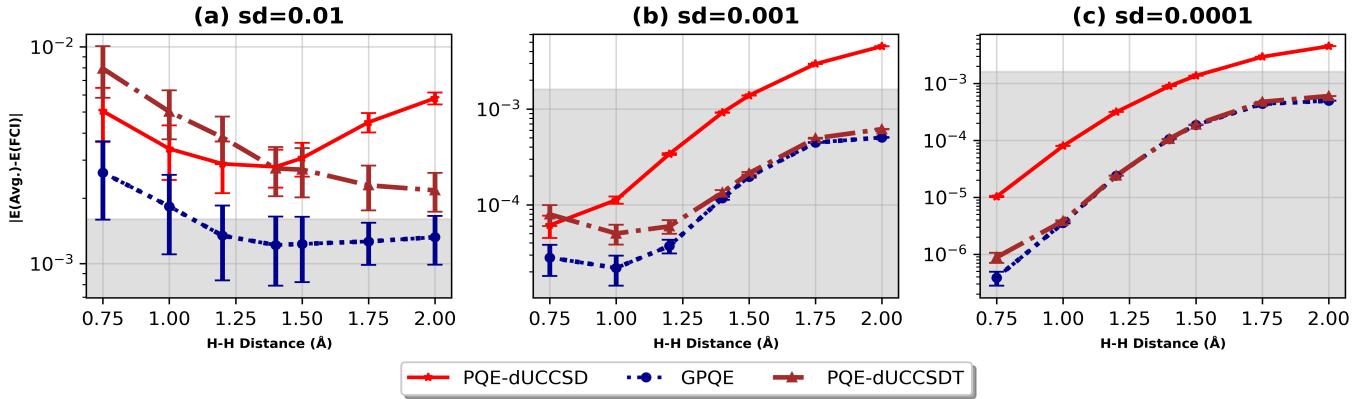


FIG. 3: Accuracy in energy with respect to FCI is plotted at several internuclear geometries for linear H_4 under Gaussian noise model characterized by standard deviation (sd) (a) 10^{-2} , (b) 10^{-3} and (c) 10^{-4} . At each geometry, the energy is averaged over 100 independent samples under Gaussian noise and error bars denote the standard deviation.

scatters and cluster operators appear only once. In a future endeavour, we will be extending our methodology to solve for cases where the operators appear more than once.

D. Simulation with a Gaussian Noise Model: Superior Accuracy over dUCCSDT-PQE

The demonstrated accuracy of our method compared to PQE-dUCCSDT under ideal noiseless environment (with the former requiring at least 1-2 orders of magnitude less quantum resources) corroborates the balanced treatment of correlation over the potential energy profiles. However, with the present devices plagued by different sources of hardware noise, the improved performance of our method still needs to be validated under actual or simulated hardware noise. With sufficiently large number of experiments performed in NISQ devices, the measurement outcomes of an observable may be faithfully sampled by a Gaussian distribution around its optimal value. Toward this, for each set of optimal parameters generated under the ideal noiseless conditions, we simulate 100 sets of noisy parameter samples by applying a Gaussian distribution model^{54,56}. Centered around the optimized PQE parameters (θ_{opt}), these noisy parameters (θ_{noisy}) are distributed according to a Gaussian model with a definite standard deviation (sd).

$$\theta_{noisy} \leftarrow \exp\left(-\frac{\theta - \theta_{opt}}{2(sd)^2}\right) \quad (16)$$

One note that this noise model may not fully account for more complex or device-specific errors such as decoherence. In our study, we have considered three different standard deviations, $sd = 10^{-2}$, 10^{-3} and 10^{-4} to represent three different noise strengths and tested the accuracy of various ansätze over the linear H_4 potential energy profile. Fig. 3 conspicuously demonstrates better noise-resilience of GPQE compared to PQE-dUCCSD and PQE-dUCCSDT ansätze. Even under significant noise strength of $sd = 10^{-2}$, the energy calculated using GPQE lies within chemical accuracy while PQE-dUCCSD

and PQE-dUCCSDT deviates substantially, justifying its superior noise-resilience within PQE family of methods.

E. Numerical Simulation with a Depolarizing Noise Channel: Superior Noise Resilience of GPQE over VQE

While our GPQE approach opens up a new direction to treat generalized operators in the projective framework that leads to less quantum resource utilization over allied PQE family of methods, such a strategy often leads to nearly identical results when the parameters are variationally optimized in the noiseless VQE framework (Fig.2). Thus the absolute superiority of our approach over VQE with an equivalently parametrized ansatz warrants further numerical validation under the realistic noisy environment. To this end, we simulated the ansatz within both VQE and GPQE frameworks with one- and two-qubit depolarizing noise channels, which can mathematically model the primary source of errors in NISQ hardware. We applied one- and two-qubit depolarizing errors of the order of 10^{-5} and 10^{-4} , respectively, and simulated the linear H_4 model at $R_{H-H} = 1.5\text{\AA}$ and BH at $R_{B-H} = 2\text{\AA}$ by averaging over 20 independent circuit runs.

Dramatically, as shown in Fig.4, even under such low intensity of noise, the optimized GPQE energy is significantly lower than the optimized VQE energy. Interestingly, the GPQE energy optimization trajectory exhibits a noticeably steeper convergence dip, in both the cases as compared to VQE. Consequently, in both Fig.4(a) and (b), GPQE shows consistently better average energy predictions with much less standard deviation than its VQE counterpart. Another interesting observation is that, in Fig.4(a) the energy of the PQE-dUCCSDT ansatz is much higher than that of both PQE-dUCCSD and GPQE, as expected, owing to the larger number of two-qubit gates in the dUCCSDT ansatz. Due to this the PQE-dUCCSDT trajectory for Fig.4(b) is not explicitly shown as it lies way above the scale of the plot along y-axis. In Fig. 4(a) we observe that PQE-dUCCSD energy profile lies close (although slightly higher, consistently) to that of our method,

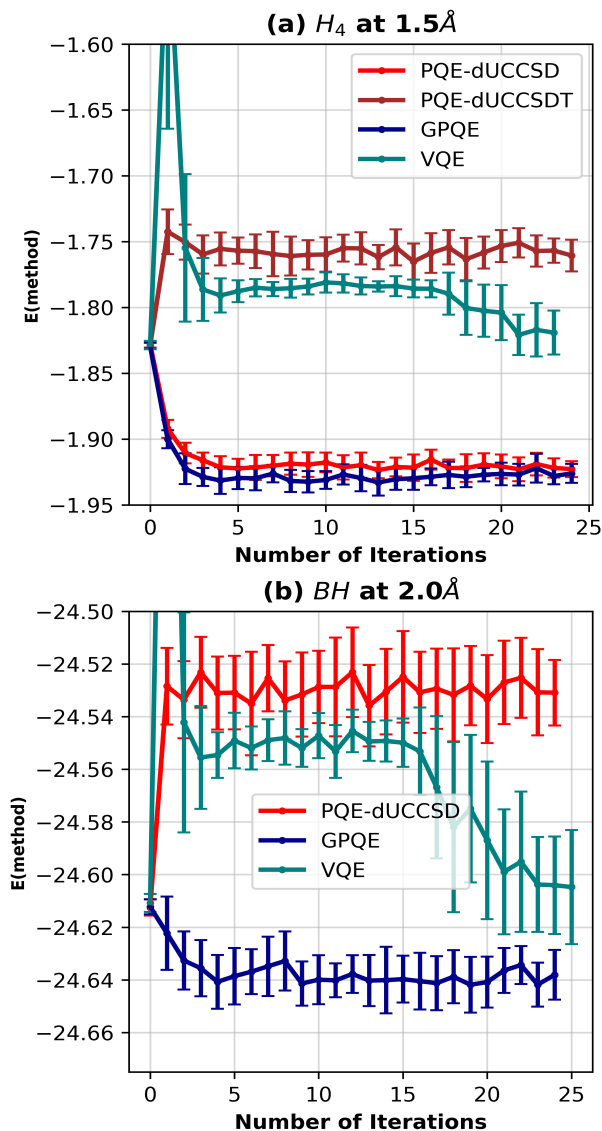


FIG. 4: Energy is plotted at each iteration under depolarizing noise channel. This energy is averaged over 20 independent runs and error bar denotes the standard deviation.

contrary to the noiseless behaviour (shown in Fig.2). Such an improved performance of PQE-dUCCSD (compared to our approach and over PQE-dUCCSDT in particular) is artificial due to being less perturbed by noise and is not due to the capture of adequate correlation effects. However, in case of Fig.4(b) as the number of CNOT gates are substantially high for PQE-dUCCSD, huge accumulation of noise affects the energy computations in a way that it does not even show any sign of convergence as can be seen from the relative behaviour of the trajectories. Thus while we may expect to have improved fault-tolerance of quantum device over next few decades, such noisy energy profile would gradually approach to their corresponding noise-free limits as given by Fig. 2 for which right numerical trend is solely dictated by the amount of correlation

captured by the theory. In this context, our method shows the best compromise between accuracy and resource efficiency in its noiseless limit while maintaining requisite accuracy in present day's noisy architecture. More importantly, in the current noisy architecture, the improved performance of GPQE over VQE convincingly demonstrates the former's robustness and superior noise resilience.

IV. CONCLUSIONS AND FUTURE OUTLOOKS:

In this manuscript, we have developed a methodology, GPQE, for determining the amplitudes corresponding to the generalized operators within the projective quantum eigensolver framework. Given the existence of the vacuum annihilating condition of the generalized operators when acted on the HF reference, the conventional Hilbert-space projection based PQE required to deal with only excitation type of operators which rapidly incurs high computational expenses due to the inclusion of high-rank excitations to achieve chemical accuracy for strongly correlated systems. In GPQE, we bypassed this issue by projecting the effective Hamiltonian against a set of contracted excited determinants, the number of which precisely equals the number of generalized unknown parameters. The residue determining equations are shown to be easily implemented in quantum computers in terms of the sum of diagonal expectation values, somewhat akin to the traditional formulation.

The solution of the generalized operators with GPQE opens up a new research direction in which one can maintain minimal circuit depth to simulate electronic strong correlation within PQE framework while concurrently retaining its high noise resilience in NISQ architecture. The advantage of this development is demonstrated under ideal environment where GPQE with a parametrized double unitary ansatz, containing both excitation and generalized operators, and is shown to be as accurate as dUCCSDT-PQE while the former requires orders of magnitude less quantum resources. This is also shown to be more accurate than dUCCSD-PQE and dUCCSDT-PQE when simulated under a Gaussian noise model. More importantly, when simulated under synthetic depolarising noise channel, GPQE is shown to be more resilient than dUCCSD-PQE, dUCCSDT-PQE and VQE (with similar ansatz), demonstrating its potential as an alternative to VQE to simulate atoms and molecules with chemistry inspired ansatz in near-term quantum computers.

A CNOT-efficient implementation of GPQE would be a good simulation protocol towards accurate determination of molecular energetics under NISQ devices. Furthermore, one may integrate various error mitigation schemes for its practical realization.

V. ACKNOWLEDGEMENT

DM thanks Prime Minister's Research Fellowship (PMRF), Government of India for his research fellowship. CP acknowledges University Grants Commission (UGC) and DH

thanks Industrial Research and Consultancy Center (IRCC), IIT Bombay for their research fellowships.

AUTHOR DECLARATIONS

Conflict of Interest:

The authors have no conflict of interests to disclose.

DATA AVAILABILITY

The numerical data that support the findings of this study are available from the corresponding author upon reasonable request.

REFERENCES

- D. S. Abrams and S. Lloyd, "Quantum algorithm providing exponential speed increase for finding eigenvalues and eigenvectors," *Phys. Rev. Lett.* **83**, 5162–5165 (1999).
- S. McArdle, S. Endo, A. Aspuru-Guzik, S. C. Benjamin, and X. Yuan, "Quantum computational chemistry," *Rev. Mod. Phys.* **92**, 015003 (2020).
- J. I. Colless, V. V. Ramasesh, D. Dahlen, M. S. Blok, M. E. Kimchi-Schwartz, J. R. McClean, J. Carter, W. A. de Jong, and I. Siddiqi, "Computation of molecular spectra on a quantum processor with an error-resilient algorithm," *Phys. Rev. X* **8**, 011021 (2018).
- C. Hempel, C. Maier, J. Romero, J. McClean, T. Monz, H. Shen, P. Jurcevic, B. P. Lanyon, P. Love, R. Babbush, A. Aspuru-Guzik, R. Blatt, and C. F. Roos, "Quantum chemistry calculations on a trapped-ion quantum simulator," *Phys. Rev. X* **8**, 031022 (2018).
- A. Peruzzo, J. McClean, P. Shadbolt, M.-H. Yung, X.-Q. Zhou, P. J. Love, A. Aspuru-Guzik, and J. L. O'Brien, "A variational eigenvalue solver on a photonic quantum processor," *Nat. Commun.* **5** (2014).
- J. Tilly, H. Chen, S. Cao, D. Picozzi, K. Setia, Y. Li, E. Grant, L. Wossnig, I. Rungger, G. H. Booth, and J. Tennyson, "The variational quantum eigensolver: A review of methods and best practices," *Phys. Rep.* **986**, 1–128 (2022).
- A. Anand, P. Schleich, S. Alperin-Lea, P. W. K. Jensen, S. Sim, M. Díaz-Tinoco, J. S. Kottmann, M. Degroote, A. F. Izmaylov, and A. Aspuru-Guzik, "A quantum computing view on unitary coupled cluster theory," *Chem. Soc. Rev.* **51**, 1659–1684 (2022).
- J. R. McClean, J. Romero, R. Babbush, and A. Aspuru-Guzik, "The theory of variational hybrid quantum-classical algorithms," *New Journal of Physics* **18**, 023023 (2016).
- T.-C. Yen, V. Verteletskyi, and A. F. Izmaylov, "Measuring all compatible operators in one series of single-qubit measurements using unitary transformations," *Journal of Chemical Theory and Computation* **16**, 2400–2409 (2020), pMID: 32150412, <https://doi.org/10.1021/acs.jctc.0c00008>.
- V. Verteletskyi, T.-C. Yen, and A. F. Izmaylov, "Measurement optimization in the variational quantum eigensolver using a minimum clique cover," *The Journal of Chemical Physics* **152**, 124114 (2020), https://pubs.aip.org/aip/jcp/article-pdf/doi/10.1063/1.5141458/15573883/124114_1_online.pdf.
- P. Gokhale, O. Angiuli, Y. Ding, K. Gui, T. Tomesh, M. Suchara, M. Martonosi, and F. T. Chong, " $\rho(n^2)$ measurement cost for variational quantum eigensolver on molecular hamiltonians," *IEEE Transactions on Quantum Engineering* **1**, 1–24 (2020).
- P. Gokhale, O. Angiuli, Y. Ding, K. Gui, T. Tomesh, M. Suchara, M. Martonosi, and F. T. Chong, "Minimizing state preparations in variational quantum eigensolver by partitioning into commuting families," (2019), arXiv:1907.13623 [quant-ph].
- W. J. Huggins, J. R. McClean, N. C. Rubin, Z. Jiang, N. Wiebe, K. B. Whaley, and R. Babbush, "Efficient and noise resilient measurements for quantum chemistry on near-term quantum computers," *npj Quantum Information* **7**, 23 (2021).
- A. F. Izmaylov, T.-C. Yen, and I. G. Ryabinkin, "Revising the measurement process in the variational quantum eigensolver: is it possible to reduce the number of separately measured operators?" *Chem. Sci.* **10**, 3746–3755 (2019).
- V. Verteletskyi, T.-C. Yen, and A. F. Izmaylov, "Measurement optimization in the variational quantum eigensolver using a minimum clique cover," *The Journal of Chemical Physics* **152**, 124114 (2020), https://pubs.aip.org/aip/jcp/article-pdf/doi/10.1063/1.5141458/15573883/124114_1_online.pdf.
- H. Singh, S. Majumder, and S. Mishra, "Sharc-vqe: Simplified hamiltonian approach with refinement and correction enabled variational quantum eigensolver for molecular simulation," (2024), arXiv:2407.12305 [quant-ph].
- M. Schuld, V. Bergholm, C. Gogolin, J. Izaac, and N. Killoran, "Evaluating analytic gradients on quantum hardware," *Phys. Rev. A* **99**, 032331 (2019).
- L. Banchi and G. E. Crooks, "Measuring Analytic Gradients of General Quantum Evolution with the Stochastic Parameter Shift Rule," *Quantum* **5**, 386 (2021).
- J. S. Kottmann, A. Anand, and A. Aspuru-Guzik, "A feasible approach for automatically differentiable unitary coupled-cluster on quantum computers," *Chem. Sci.* **12**, 3497–3508 (2021).
- N. H. Stair and F. A. Evangelista, "Simulating many-body systems with a projective quantum eigensolver," *PRX Quantum* **2**, 030301 (2021).
- F. A. Evangelista, G. K.-L. Chan, and G. E. Scuseria, "Exact parameterization of fermionic wave functions via unitary coupled cluster theory," *The Journal of Chemical Physics* **151**, 244112 (2019), https://pubs.aip.org/aip/jcp/article-pdf/doi/10.1063/1.5133059/16659468/244112_1_online.pdf.
- I. Magoulas and F. A. Evangelista, "Cnot-efficient circuits for arbitrary rank many-body fermionic and qubit excitations," *Journal of Chemical Theory and Computation* **19**, 822–836 (2023).
- Y. S. Yordanov, D. R. Arvidsson-Shukur, and C. H. Barnes, "Efficient quantum circuits for quantum computational chemistry," *Physical Review A* **102**, 062612 (2020).
- K. Kowalski and P. Piecuch, "The method of moments of coupled-cluster equations and the renormalized ccSD [t], ccSD (t), ccSD (tq), and ccSDt (q) approaches," *The Journal of Chemical Physics* **113**, 18–35 (2000).
- I. Magoulas and F. A. Evangelista, "Unitary coupled cluster: Seizing the quantum moment," *The Journal of Physical Chemistry A* **127**, 6567–6576 (2023).
- C. Patra, S. Halder, and R. Maitra, "Projective quantum eigensolver via adiabatically decoupled subsystem evolution: A resource efficient approach to molecular energetics in noisy quantum computers," *The Journal of Chemical Physics* **160** (2024).
- S. Halder, C. Patra, D. Mondal, and R. Maitra, "Machine learning aided dimensionality reduction toward a resource efficient projective quantum eigensolver: Formal development and pilot applications," *The Journal of Chemical Physics* **158** (2023).
- C. Patra, D. Mukherjee, S. Halder, D. Mondal, and R. Maitra, "Towards a resource-optimized dynamic quantum algorithm via non-iterative auxiliary subspace corrections," arXiv preprint arXiv:2408.12944 (2024).
- C. Patra, V. Agarwal, D. Halder, A. Chakraborty, D. Mondal, S. Halder, and R. Maitra, "A synergistic approach towards optimization of coupled cluster amplitudes by exploiting dynamical hierarchy," *ChemPhysChem* **24**, e202200633 (2023).
- V. Agarwal, C. Patra, and R. Maitra, "An approximate coupled cluster theory via nonlinear dynamics and synergetics: The adiabatic decoupling conditions," *The Journal of Chemical Physics* **155** (2021).
- J. Lee, W. J. Huggins, M. Head-Gordon, and K. B. Whaley, "Generalized unitary coupled cluster wave functions for quantum computation," *J. Chem. Theory Comput.* **15**, 311–324 (2018).
- D. Halder, V. S. Prasanna, and R. Maitra, "Dual exponential coupled cluster theory: Unitary adaptation, implementation in the variational quantum eigensolver framework and pilot applications," *J. Chem. Phys.* **157**, 174117 (2022).

- ³³R. Maitra, Y. Akinaga, and T. Nakajima, "A coupled cluster theory with iterative inclusion of triple excitations and associated equation of motion formulation for excitation energy and ionization potential," *J. Chem. Phys.* **147**, 074103 (2017).
- ³⁴S. Tribedi, A. Chakraborty, and R. Maitra, "Formulation of a dressed coupled-cluster method with implicit triple excitations and benchmark application to hydrogen-bonded systems," *J. Chem. Theory Comput.* **16**, 6317–6328 (2020).
- ³⁵A. Chakraborty and R. Maitra, "Fixing the catastrophic breakdown of single reference coupled cluster theory for strongly correlated systems: Two paradigms toward the implicit inclusion of high-rank correlation with low-spin channels," *The Journal of Chemical Physics* **159**, 024106 (2023), https://pubs.aip.org/aip/jcp/article-pdf/doi/10.1063/5.0146765/18037101/024106_1_5.0146765.pdf.
- ³⁶M. Nooijen and V. Lotrich, "Brueckner based generalized coupled cluster theory: Implicit inclusion of higher excitation effects," *The Journal of Chemical Physics* **113**, 4549–4557 (2000), https://pubs.aip.org/aip/jcp/article-pdf/113/11/4549/19320262/4549_1_online.pdf.
- ³⁷D. W. Berry, C. Gidney, M. Motta, J. R. McClean, and R. Babbush, "Qubitization of arbitrary basis quantum chemistry leveraging sparsity and low rank factorization," *Quantum* **3**, 208 (2019).
- ³⁸M. Nooijen, "Can the eigenstates of a many-body hamiltonian be represented exactly using a general two-body cluster expansion?" *Phys. Rev. Lett.* **84**, 2108–2111 (2000).
- ³⁹H. Nakatsuji, "Equation for the direct determination of the density matrix," *Phys. Rev. A* **14**, 41–50 (1976).
- ⁴⁰D. A. Mazziotti, "Contracted schrödinger equation: Determining quantum energies and two-particle density matrices without wave functions," *Phys. Rev. A* **57**, 4219–4234 (1998).
- ⁴¹D. Halder, S. Halder, D. Mondal, C. Patra, A. Chakraborty, and R. Maitra, "Corrections beyond coupled cluster singles and doubles through selected generalized rank-two operators: digital quantum simulation of strongly correlated systems," *Journal of Chemical Sciences* **135**, 41 (2023).
- ⁴²T. Q. N. developers and contributors, "Qiskit nature 0.6.0," (2023).
- ⁴³Q. Sun, T. C. Berkelbach, N. S. Blunt, G. H. Booth, S. Guo, Z. Li, J. Liu, J. D. McClain, E. R. Sayfutyarova, S. Sharma, S. Wouters, and G. K.-L. Chan, "Pyscf: the python-based simulations of chemistry framework," *WIREs Comput. Mol. Sci.* **8**, e1340 (2018).
- ⁴⁴W. J. Hehre, R. F. Stewart, and J. A. Pople, "Self-consistent molecular-orbital methods. i. use of gaussian expansions of slater-type atomic orbitals," *J. Chem. Phys.* **51**, 2657–2664 (1969).
- ⁴⁵J. T. Seeley, M. J. Richard, and P. J. Love, "The bravyi-kitaev transformation for quantum computation of electronic structure," *J. Chem. Phys.* **137**, 224109 (2012).
- ⁴⁶P. Pulay, "Convergence acceleration of iterative sequences. the case of scf iteration," *Chemical Physics Letters* **73**, 393–398 (1980).
- ⁴⁷C. G. BROYDEN, "The Convergence of a Class of Double-rank Minimization Algorithms: 2. The New Algorithm," *IMA Journal of Applied Mathematics* **6**, 222–231 (1970), <https://academic.oup.com/imamat/article-pdf/6/3/222/1848059/6-3-222.pdf>.
- ⁴⁸R. Fletcher, "A new approach to variable metric algorithms," *The Computer Journal* **13**, 317–322 (1970), <https://academic.oup.com/comjnl/article-pdf/13/3/317/988678/130317.pdf>.
- ⁴⁹D. Goldfarb, "A family of variable-metric methods derived by variational means," *Math. Comp.* **24**, 23–26 (1970).
- ⁵⁰D. F. Shanno, "Conditioning of quasi-Newton methods for function minimization," *Math. Comp.* **24**, 647–656 (1970).
- ⁵¹P. Virtanen, R. Gommers, T. E. Oliphant, M. Haberland, T. Reddy, D. Cournapeau, E. Burovski, P. Peterson, W. Weckesser, J. Bright, and *et al.*, "Scipy 1.0: fundamental algorithms for scientific computing in python," *Nature Methods* **17**, 261–272 (2020).
- ⁵²N. H. Stair and F. A. Evangelista, "Qforte: an efficient state simulator and quantum algorithms library for molecular electronic structure," arXiv preprint arXiv:2108.04413 (2021).
- ⁵³D. Halder, D. Mondal, and R. Maitra, "Noise-independent route toward the genesis of a COMPACT ansatz for molecular energetics: A dynamic approach," *The Journal of Chemical Physics* **160**, 124104 (2024), https://pubs.aip.org/aip/jcp/article-pdf/doi/10.1063/5.0198277/19844810/124104_1_5.0198277.pdf.
- ⁵⁴D. Mondal, D. Halder, S. Halder, and R. Maitra, "Development of a compact Ansatz via operator commutativity screening: Digital quantum simulation of molecular systems," *J. Chem. Phys.* **159**, 014105 (2023).
- ⁵⁵S. Halder, A. Dey, C. Shrikhande, and R. Maitra, "Machine learning assisted construction of a shallow depth dynamic ansatz for noisy quantum hardware," *Chem. Sci.* **15**, 3279–3289 (2024).
- ⁵⁶O. R. Meitei, B. T. Gard, G. S. Barron, D. P. Pappas, S. E. Economou, E. Barnes, and N. J. Mayhall, "Gate-free state preparation for fast variational quantum eigensolver simulations," *npj Quantum Inf.* **7**, 155 (2021).